EMBRYO BIOLOGY

Dysfunction in gap junction intercellular communication induces aberrant behavior of the inner cell mass and frequent collapses of expanded blastocysts in mouse embryos

Kazue Togashi[1] · Jin Kumagai[1] · Emiko Sato[1] ·
Hiromitsu Shirasawa[1] · Yuki Shimoda[1] · Kenichi Makino[1] · Wataru Sato[1] ·
Yukiyo Kumazawa[1] · Yasufumi Omori[2] · Yukihiro Terada[1]

Abstract

Purpose We investigated the role of gap junctions (GJs) in embryological differentiation, and observed the morphological behavior of the inner cell mass (ICM) by time-lapse movie observation (TLM) with gap junction inhibitors (GJis).

Methods ICR mouse embryos were exposed to two types of GJis in CZB medium: oleamide (0 to 50 μM) and 1-heptanol (0 to 10 mM). We compared the rate of blastocyst formation at embryonic day 4.5 (E4.5) with E5.5. We also observed and evaluated the times from the second cleavage to each embryonic developing stage by TLM. We investigated embryonic distribution of DNA, Nanog protein, and Connexin 43 protein with immunofluorescent staining.

Results In the comparison of E4.5 with E5.5, inhibition of gap junction intercellular communication (GJIC) delayed embryonic blastocyst formation. The times from the second cleavage to blastocyst formation were significantly extended in the GJi-treated embryos (control vs with oleamide, 2224 ± 179 min vs 2354 ± 278 min, $p=0.013$). Morphological differences were traced in control versus GJi-treated embryos until the hatching stage. Oleamide induced frequent severe collapses of expanded blastocysts (77.4 % versus 26.3 %, $p=0.0001$) and aberrant ICM divisions connected to sticky strands (74.3 % versus 5.3 %, $p=0.0001$). Immunofluorescent staining indicated Nanog-positive cells were distributed in each divided ICM.

Conclusions GJIC plays an important role in blastocyst formation, collapses of expanded blastocysts, and the ICM construction in mouse embryos.

Keywords Gap junction inhibitor · Time-lapse movie observation · Delayed blastocyst formation · Blastocoel collapse · ICM division

Introduction

The cooperation among blastomeres plays a key role in the process of embryonic differentiation. Each blastomere can be easily distinguished until compaction occurs with increased adhesion of the blastomeres. Embryos with their compactions disrupted by an anti-E-cadherin monoclonal antibody have impaired differentiation [1, 2]. These results suggest that adhesions of blastomeres themselves are important for differentiation. The cell-to-cell communication or the signaling among blastomeres might be more important as compared with cell-to-cell adhesions in embryonic differentiation. Gap junctions (GJs) are involved in direct signal transduction between adhering adjacent blastomeres. Gap junction intercellular communication (GJIC) transmits various signals including activation of the Hippo signaling pathway, which is associated with differentiation of the trophectoderm (TE) / inner cell mass (ICM) [3]. GJs have also been suggested to play a role in blastocoel formation of the preimplantation embryo [4].

GJs, composed of various combinations of connexin (Cx) subtypes, are made of two hemi-channels consisting of hexamers of the four-trans membrane protein Cx. Preimplantation embryos express multiple connexins and assemble them into GJs. Cx30, Cx30.3, Cx31, Cx31.1, Cx36, Cx40, Cx43, Cx45, and Cx57 express to a preimplantation mouse embryo, but not Cx26 and Cx32 [5]. Transcription factors of Cx26, Cx31, Cx43, and Cx45 were detected in human embryos. Cx43, in particular, was indicated in all embryonic developing stages [6]. Cx knockout (KO) mice, however, have produced phenotypes that go against previous predictions. Although neonates died of a heart anomaly, Cx43KO mice were term birth. Females with dominant inactivating mutations in the gene GJA1, which encodes Cx43, are also generally fertile. These findings suggest directly opposed ideas. Co-expressing connexins may compensate for one another and Cx43 may have no critical role in the reproductive system [7]. Nevertheless, it has been suggested that Cx43 is involved in acquisition of pluripotency in ES cells and iPS cells [8]. It is still controversial whether the embryonic role of Cx43 is essential or not.

Embryonic GJIC was confirmed from a compaction embryo in the 8-cell period [9], and was observed cells that presented ICM at the blastocyst stage in mouse embryos [10]. Developmental impairment of mouse embryo was reported in some studies using connexin antibodies or antisense RNA injections to disrupt GJIC. The absence of GJIC reduces blastocyst incidence in mice, which naturally exhibit reduced cell-to-cell communication (DDK syndrome) [11]. Though it is expected to depend on gap junctions, pharmacologic inhibitors of GJIC have no effect on blastocyst development [12]. These discrepancies remain unresolved [4, 7].

Time-lapse movie observation (TLM) provides morphological information. Mio & Maeda reported thought-provoking findings of human embryos that formed two ICMs connected to the sticky strand after a collapse and re-expansion of the cavity [13]. There is speculation that an aberrant ICM split in in vitro freeze/thaw human embryos could be a phenotype of differentiation deficiency. They also speculated on the relationship between such a morphological blastocyst phenomenon and the risk of monozygotic twin pregnancy. To date, additional experiments to prove these speculations have not been carried out.

We hypothesized that ICM construction was associated with GJIC. And we aimed at evaluating the roles of GJs in embryonic differentiation and morphological behavior. Even though it is suggested that GJs are associated with embryonic development and differentiation, there have been few reports regarding the preimplantation embryonic morphology. TLM observation, which has never been used in embryonic GJIC experiments, was adopted in our study. Oleamide or 1-heptanol, which has been used as a common low-toxic GJ inhibitor (GJi) in somatic cells, was also adopted.

Materials and methods

Retrieval of preimplantation mouse embryo

This study was approved by the Institutional Animal Care and Use Committee (Permission number: 26-1-49) and carried out according to the Akita University Animal Experimentation Regulations. Female ICR mice (CLEA Japan, Tokyo, Japan and Japan SLC, Shizuoka, Japan) aged 8–12 weeks old were intraperitoneally injected with human menopausal gonadotropin (Pergogreen, Serono Laboratories, Geneva, Switzerland) and human chorionic gonadotropin (HCG Mochida, Mochida Pharmaceutical Co, Tokyo, Japan) to induce ovulation. We mated those mice and confirmed vaginal plug in each female mouse. At embryonic day 1.5 (E1.5), we retrieved mice embryos by perfusing the oviducts of mated female mice with modified HTF medium (NK system, Osaka, Japan) containing 10 % fetal bovine serum (Life Technologies, Carlsbad, USA). Preimplantation embryos were collected at the 2-cell stage.

Embryo culture

Retrieved embryos were cultured with ×1 EmbryoMax™ CZB Medium with Phenol Red (Merck Millipore, Darmstadt, Germany) supplemented with the following GJis: oleamide (Sigma-Aldrich, St. Louis, USA) at a concentration of 5, 10, 20, or 50 μM and 1-heptanol (Wako Pure Chemical, Osaka, Japan) at a concentration of 0.1, 1, 5, or 10 mM. Up to 10 embryos were co-cultured in a 100-μl drop of medium on a BD Falcon Easy-Grip™ Tissue Culture Dish (BD Biosciences, Bedford, USA), which was covered with mineral oil. GJis were dissolved in DMSO (Wako Pure Chemical), and all mediums for embryo culture were adjusted to 0.1 % DMSO as the final concentration. Embryo culture conditions were as follows: 5 % O_2, 5 % CO_2, 90 % N_2, and 37.5 °C. Culture mediums were not replaced during the experiments.

Observations of the developing embryos

We observed the embryonic morphology under a microscope (BX53P DP73, Olympus, Tokyo, Japan) on embryonic day 4.5 (E4.5, 479 total embryos) or embryonic day 5.5 (E5.5, 112 total embryos). We observed each embryo and compared them by the rate of blastocyst formation.

Immunofluorescence staining of embryos

Embryos were fixed in 4 % formaldehyde (Cosmo Bio, Tokyo, Japan) in D-PBS (Sigma-Aldrich) for 15 min after observation and measurement. The embryos were incubated for 40 min in transmission solution, i.e., D-PBS (+$MgSO_4$+$CaCl_2$) containing 0.2 % Triton-X (Sigma-Aldrich) and 0.1 %

Tween-20 (Sigma-Aldrich), after washing three times for 5 min in wash buffer-1, i.e., D-PBS ($+MgSO_4+CaCl_2$) with 0.3 % BSA (product of New Zealand, Wako Pure Chemical). They were then washed three times for 5 min in wash buffer-2, i.e., D-PBS ($+MgSO_4+CaCl_2$) with 0.05 % Tween-20. After blocking using wash buffer-2 with 2 % goat serum, embryos were incubated overnight at 4 °C in primary antibody solution that contained mouse monoclonal anti-Cx43 (20369933, ZYMED, Sun Francisco, USA) and rabbit polyclonal anti-Nanog (ab80892, Abcam, Cambridge, UK) antibodies. Both antibodies were diluted 1:1000. They were washed three times for 5 min in wash buffer-2 and placed in secondary antibody solution for 40 min at room temperature and shielded from light, and then washed three times for 5 min in wash buffer-2. The secondary antibody solution contained a mixture of Alexa Flour 488–conjugated goat anti–mouse IgG (Invitrogen, Carlsbad, USA), diluted 1:500, and Alexa Flour 546–conjugated goat anti–rabbit IgG (Invitrogen), diluted 1:1000. The stained embryos were placed in 10–40 % glycerol (Wako Pure Chemical) to prevent distortion. Hoechst 33342 buffer (Dojindo Molecular Technologies, Kumamoto, Japan) was used to stain embryonic DNA for 20 min. A negative control mouse embryo was prepared using the same protocol without placing it in primary antibody solution.

The stained embryos were observed and measured on a BX53P DP73 fluorescence microscope (Olympus) and an LSM780 confocal laser–scanning microscope (Carl Zeiss AG, Jena, Germany).

Time –lapse movie observation and analysis

Mouse embryos (161 total embryos) were cultured in a time-lapse incubator in CZB medium with/without 50 µM oleamide or 10 mM 1-heptanol. Up to 10 embryos were co-cultured in a 100-µl drop of medium on embryo GPS® dishware (LifeGrobal, Guelph, Canada), which was covered with mineral oil. Embryo culture conditions were as follows: 5 % O_2, 5 % CO_2, 90 % N_2, and 37.5 °C. We took images of cultured embryos from E1.5 to E5.5 (5760 min) every 3 min by TLM using the CCM-IVF & CCM-M1.4 software (ASTEC). We measured the time the embryo spent on growing from second cleavage to each differential stage. We tracked the morphological development and behavior of all observable embryos (141 total embryos) and counted those with 'complete collapse,' in which the blastocoel was completely collapsed, and 'severe collapse,' in which the volume of the blastocoel was collapsed by more than 30 %, as in a previous report [14]. We observed each embryo and compared them by the rate of blastocyst formation. We also observed the phenomenon of 'ICM division,' in which sticky strands emerged between ICMs after blastocyst formation.

Preparation of discarded human blastocysts

We acquired discarded blastocysts from patients who had undergone in vitro fertilization and embryo transfer in our hospital, with the approval of the ethical review board of our hospital and Japan Society of Obstetrics and Genecology. Frozen blastocysts were thawed using the Cryotop Safety Kit (Kitazato Bio Pharma, Shizuoka, Japan), and those blastocysts were cultured in Blast Assist medium (Origio, Måløv, Denmark) for recovery. Up to four embryos were co-cultured in a 100-µl drop of medium on an embryo GPS® dish (LifeGrobal), which was covered with mineral oil. Embryo culture conditions were as follows: 5 % O_2, 5 % CO_2, 90 % N_2, and 37.5 °C. Blastocysts were observed by TLM every 3 min using the CCM-IVF & CCM-M1.4 software (ASTEC).

Results

Influence of GJis on embryonic development

Blastocyst formation of the control (cultured in 0.1 % DMSO) mice embryos (E4.5 vs E5.5 observation) was 87.5 % vs 90.9 % (Fig. 1a, b). The rate of blastocyst formation in embryos cultured with oleamide at concentrations of 5, 10, 20, and 50 µM (E4.5 vs E5.5) were 88.9 % vs 100 %, 84.8 % vs 90.9 %, 81.3 % vs 90.9 %, and 75.0 % vs 72.7 %, respectively (Fig. 1a, b). Blastocyst formation in embryos cultured with 50 µM oleamide at E4.5 significantly decreased ($p=0.022$) (Fig. 1a). In contrast, the rate of blastocyst formation in embryos cultured with 1-heptanol at concentrations of 0.1, 1, 5, and 10 mM (E4.5 vs E5.5) were 91.8 % vs 100 %, 87.5 % vs 90.0 %, 83.7 % vs 100 %, and 66.0 % vs 100 %, respectively (Fig. 1c, d). Blastocyst formation at E4.5 significantly decreased in the embryos cultured with 10 mM 1-heptanol ($p=0.001$) (Fig. 1c). The rate of blastocyst formation in embryos cultured with GJi decreased in a GJi concentration–dependent manner at E4.5 observation ($n=479$, Fig. 1a, c), but not at E5.5 observation ($n=112$, Fig. 1b, d).

Time –lapse movie (TLM) observation

We measured the time to each embryonic differentiation stage with the second cleavage as the starting point under culture conditions with/without 50 µM oleamide or 10 mM 1-heptanol. Compared with control embryos, the time from the second cleavage to the third cleavage of embryos cultured with oleamide or heptanol was significantly extended (Fig. 2a). Embryos cultured with heptanol showed significantly delayed compaction, even though embryos cultured with oleamide did not (Fig. 2b). The initiation of blastocoel
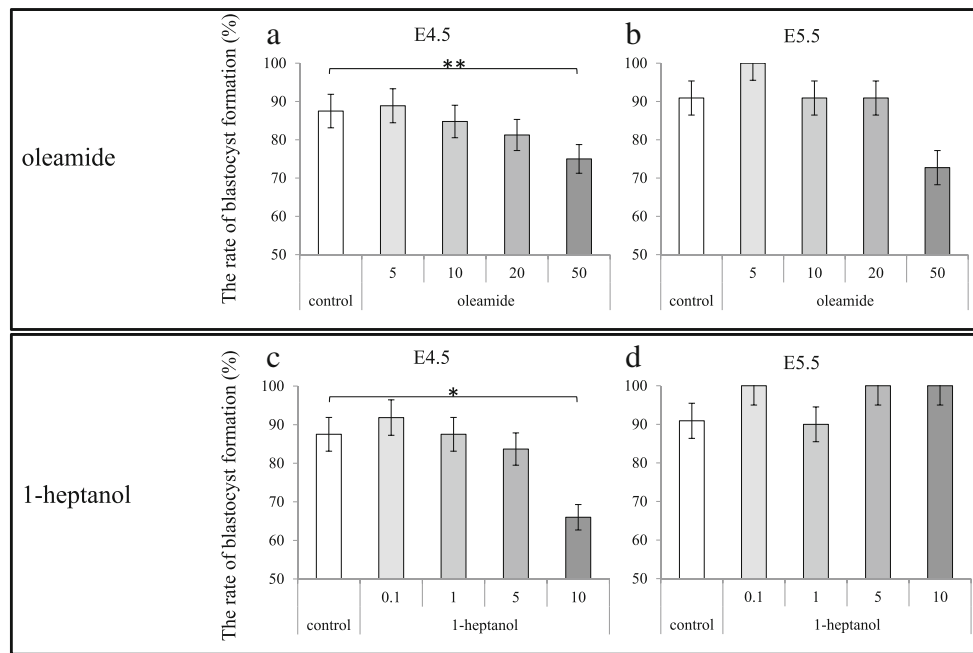
Fig. 1 GJis reduced the rate of blastocyst formation of mouse embryos at E4.5, but it caught up at E5.5. The vertical axis shows the rate of blastocyst formation. The horizontal axis shows the concentration of GJis. Oleamide was compared at a concentration of 0, 5, 10, 20, or 50 μM. 1- heptanol was compared at a concentration of 0, 0.1, 1, 5, or 10 mM. Data are means. $p<0.001$ (*), $p<0.05$ (**), for each group versus DMSO 0.1 % group as a control. **a**: The rate of blastocyst formation in embryos cultured with oleamide at E4.5. **b**: The rate of blastocyst formation in embryos cultured with oleamide at E5.5. **c**: The rate of blastocyst formation in embryos cultured with 1-heptanol at E4.5. **d**: The rate of blastocyst formation in embryos cultured with 1-heptanol at E5.5

formation was significantly extended in embryos cultured with oleamide (Fig. 2c). Finally, there were no significant differences in time to initiation of the hatching stage (Fig. 2d).

TLM observation revealed aberrant ICM division in mouse embryos cultured with GJis, resembling human freeze/thaw embryos in a cytoplasmic sticky strand (Fig. 3, supplemental movie 1A, 1B and 2). The frequency of 'ICM division' was 5.3 % (2/38) for the control embryos, 74.3 % (23/31) for the embryos cultured with oleamide ($p<0.0001$), and 65.6 % (21/32) for the embryos cultured with heptanol ($p<0.0001$). The
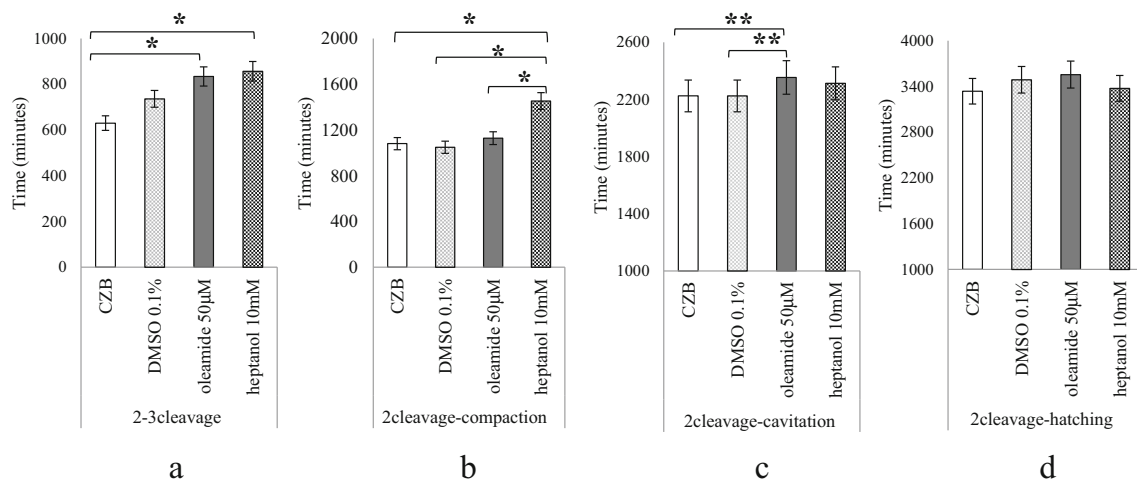

Fig. 2 GJis delayed embryonic development (TLM observation). The mean time spent from the second cleavage to third cleavage, compaction, initiation of blastocoel formation, and initiation of hatching. Embryos were cultured with CZB ($n=41$), 0.1 % DMSO ($n=37$), oleamide 50 μM ($n=43$), or heptanol 10 mM ($n=31$). The vertical axis shows total cultured minutes from the second cleavage. p-value is for oleamide or 1-heptanol versus control. $p<0.001$ (*), $p<0.05$ (**) **a**: The time from the second cleavage to the third cleavage was significantly delayed with both GJis. **b**: Though the time to compaction was not significantly different with oleamide, embryos cultured with heptanol were significantly delayed. **c**: The time to initiation of blastocoel formation was significantly longer in the presence of both GJis. **d**: The difference in the time to start of hatching was not significant at all
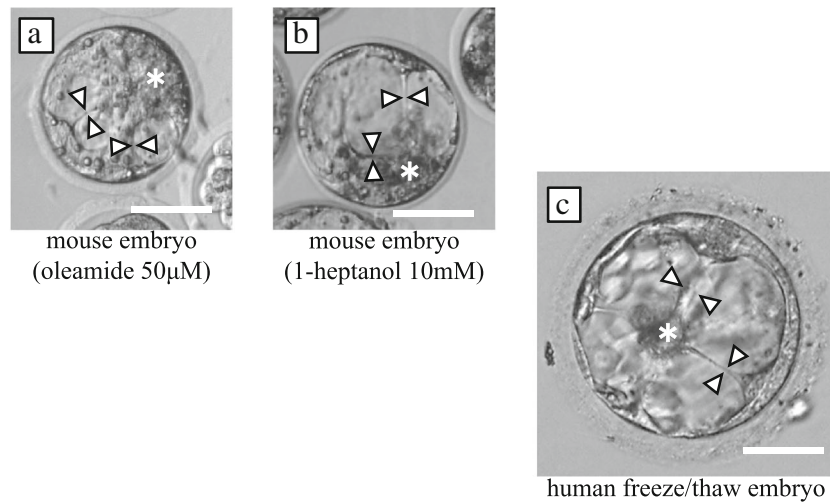
Fig. 3 Aberrant ICM divisions were observed in mouse embryos. **a**: Mouse blastocyst cultured with 50 μM oleamide. Plural strands (white arrowhead) from the ICM (*) were also observed. This aberrant ICM division was observed upon blastocoel formation. **b**: Mouse blastocyst cultured with 10 mM heptanol. Strands (white arrowhead) from the ICM (*) were observed. This aberrant ICM division was observed after a collapse. **c**: Human blastocyst frozen by vitrification on day 5, 3BB (blastocyst grading system introduced by Gardner and Schoolcraft in 1999), and thawed. Plural sticky strands (white arrowhead) from the ICM (*) were observed radially. This aberrant ICM division was observed after a collapse. Scale bar: 50 μm

'complete collapse' and 'severe collapse' were also significantly more frequent in the embryos cultured with oleamide or heptanol as compared with the control embryos. 'Severe collapse' was seen in 26.3 % (10/38) of the control embryos, 77.4 % (24/31) of the oleamide embryos ($p=0.0001$), and 87.5 % (28/32) of the heptanol embryos ($p=0.0002$). 'Complete collapse' was found in 13.2 % (5/38) of the control embryos, 29.0 % (9/31) of the oleamide embryos ($p=0.0349$), and 40.6 % (13/32) of the heptanol embryos ($p=0.0047$). There was no significant difference in the overall rates of blastocyst formation (Table 1).

Immunofluorescent staining

Mouse or human embryos were stained with DNA, Nanog protein, and Cx43 protein (Fig. 4, supplemental movie 3A and 3B). Just one ICM was constructed in mouse embryos cultured without GJis. The ICM also included Nanog-positive cells. Cx43 distribution was clear around Nanog-positive cells (Fig. 4a). In contrast, there was a strand between divided ICMs including Nanog-positive cells in the mouse embryos cultured with oleamide. The distribution of Cx43 was not specific (Fig. 4b, supplemental movie 3A). Mouse embryos cultured without GJis and stained without primary antibodies were used as a control (Fig. 4c).

Additionally, two or more ICMs including Nanog-positive cells were observed in the human freeze/thaw embryo (Fig. 4d, See supplemental movie 3B).

Discussion

Oleamide and 1-heptanol

Previous embryonic experiments commonly adopted 18-α-glycyrrhetinic acid (18-AGA) as a GJi. 18-AGA is not a

Table 1 Embryonic events observed by time-lapse movie. We observed morphological development and behavior of all embryos and classified them as 'complete collapse,' in which the blastocoel was completely collapsed, or 'severe collapse,' in which the volume of the blastocoel was reduced more than 30 %. We also observed the phenomenon of 'ICM division,' in which cytoplasmic sticky strands formed between ICMs during blastocoel formation. The frequency of blastocoel collapse and ICM division was specifically increased in the embryos cultured with GJis. Statistically analyzed by chi-square test, Fischer's exact test, and Mann–Whitney U-test, * $p < 0.0001$, **$p < 0.05$

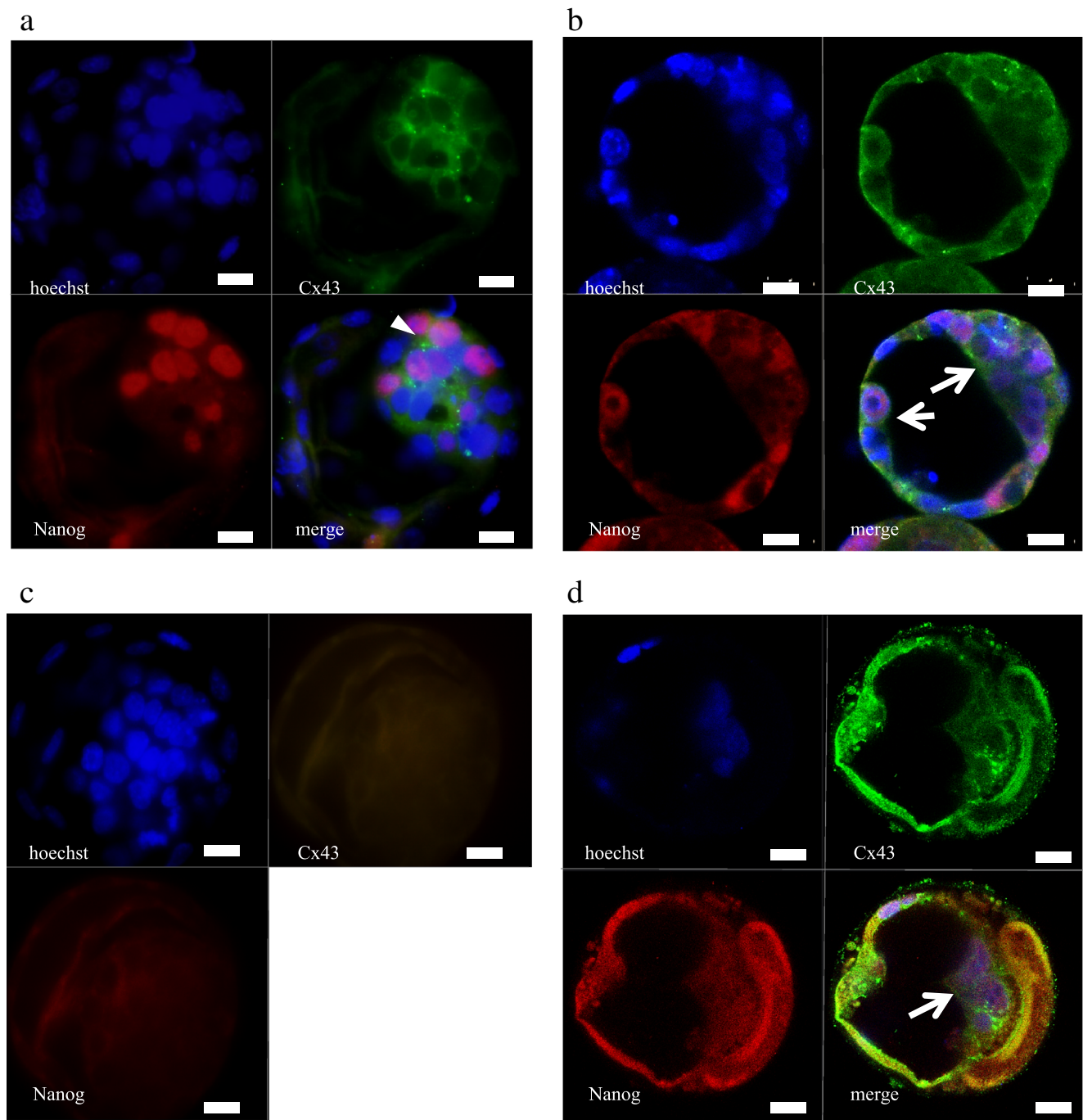|	CZB	oleamide 50 μM	1-heptanol 10 mM
complete collapse	13.2 % (5/38)	29.0 % (9/31)**	40.6 % (13/32)**
mean±SD	0.1±0.3	0.5±0.9	0.7±0.8
(range)	(0–1)	(0–3)	(0–3)
severe collapse	26.3 % (10/38)	77.4 % (24/31)*	87.5 % (28/32)**
mean±SD	0.3±0.5	4.5±5.2	5.5±7.3
(range)	(0–2)	(0–20)	(0–30)
ICM division	5.3 % (2/38)	74.3 % (23/31)*	65.6 % (21/32)*
the overall rate of blastocyst formation	97.6 % (37/38)	95.6 % (30/31)	96.9 % (31/32)

a

b

c

d

Fig. 4 Distribution of Nanog-positive cells in mouse and human embryos **a**: Mouse blastocyst cultured without GJis. Cx43 was expressed between all cells of the ICM and TE at the blastocyst stage, though more clearly between ICM, around Nanog-positive cells (white arrowhead). Nanog was expressed through the developmental stage with a mosaic pattern in ICM at the blastocyst stage. **b**: Mouse blastocyst cultured with oleamide 50 μM. Both ICMs included Nanog-positive cells (white arrows). Cx43 distribution was not as specific as mouse blastocyst cultured without GJis. This ICM behavior was observed upon cavitation. **c**: Negative control mouse blastocyst stained without primary antibody. **d**: Human blastocysts frozen on day 5, 3BC (blastocyst grading system introduced by Gardner and Schoolcraft in 1999), and thawed. Nanog was positive at the ICM (white arrow, see supplemental movie 3B). This ICM behavior was observed after a collapse. green, Cx43; red, Nanog; blue, DNA. Scale bar: 20 μm

specific GJi and indirectly blocks GJs through activation of protein kinases, G-proteins, or ATPases [15]. In the reduction of potassium signaling, 18-AGA is a concentration-dependent GJi [16]. Even though 18-AGA completely abolished dye coupling of GJIC, 18-AGA has no effect on blastocyst development [12]. Though these are expected to depend on GJIC, 18-AGA has no effect on total cell number, the ratio of cells in the TE and ICM, the distribution of energy substrates, or the

ratio of apoptotic cells within the embryo [5]. Because of such an unsolved discrepancy with 18-AGA, we explored other GJis for the current embryonic study.

Both oleamide and 1-heptanol are GJis that have been used in experiments of cultured somatic cells. Oleamide is an endogenous sleep-related lipid with low toxicity. Oleamide was found to potently and selectively inactivate gap junction–mediated communication between rat glial cells. Oleamide had no effect on mechanically stimulated calcium wave transmission [17]. 1-heptanol, an extremely stable primary alcohol with minimal toxicity, has been used as a GJi of cardiac muscle cells. 1-heptanol also inhibits sodium channels [18]. Heptanol blocked not only gap junction communication but also intercellular calcium signaling. Appropriate concentrations of both inhibitors have been reported. Complete inhibition of dye transfer was observed with 50 μM oleamide [17]. The amount of glutathione in cultured oocytes tended to decrease as the concentration of heptanol in the medium was increased. It reduced to the control level with 10 mM heptanol [19]. Therefore, we used 0 to 50 μM oleamide and 0 to 10 mM heptanol.

It was suggested that both oleamide and 1-heptanol delayed blastocoel formation dose-dependently. Additional cultivation increased the rate of blastocyst formation with the exception of embryos cultured with oleamide 50 μM (Fig. 1). Complete inhibition of GJIC might stop embryonic development. TLM observation of the developing embryos revealed the difference between oleamide and heptanol. Though the cell cycle was significantly delayed with both GJis (Fig. 2a), heptanol specifically delayed compaction (Fig. 2b). Oleamide significantly delayed blastocoel formation (Fig. 2c). These results indicate that a sodium channel or potassium channel plays some role in compaction. However, there was no difference when the TLM period extended to the initiation of hatching (Fig. 2d). Embryonic development was differently delayed with each GJi. It is suggested that developmental delay is associated with ionic environments. Further studies will be required to investigate the difference. Such findings might bring about a new understanding of the in vitro embryonic culture environment.

The aberrant ICM behavior and the cytoplasmic sticky strand

It has been suggested that GJIC dysfunction or GJis cause the aberrant split of ICM and sticky strands (Fig. 3a, b and Supplemental movie 1). This phenomenon has never been reported in mouse embryos, though a similar phenomenon was reported in human freeze/thaw embryos [13]. The phenomenon of human freeze/thaw embryos morphologically resembled that of mouse embryos, which we report (Supplemental movie 1B and 2). The same phenomenon is observed in mouse embryos cultured with the two GJis (Fig. 3a, b, c). It is suggested that the reduced function of GJIC is associated with this phenomenon.

This result might serve as a clue to investigation of the role of GJIC on ICM division.

To evaluate the relation between embryonic ICM division and GJIC, embryos were stained with DNA, Nanog protein, and Cx43 protein. Nanog works together with other key pluripotent factors such as Oct4 and Sox2 to control a set of target genes that have important functions in cell pluripotency [20]. It has been suggested that Cx43 is associated with acquisition of pluripotency in ES cells and iPS cells [8, 21]. Further studies will be required to define the cellular mechanisms by which GJis associate with ICM division. Nevertheless, this result suggests the pluripotency in both sides of divided ICMs connected by a sticky strand (Fig. 4b, d and supplemental movie 3A, 3B).

Embryonic collapse and GJIC function

In the current TLM observation, mouse embryos cultured with GJi presented frequent collapses and developmental delay. Time-lapse markers provide useful information with new non-invasive methods for improving embryo selection [22]. Referring to previous studies, blastocoel collapse and developmental delay might have an association with embryo quality and hatching. Mio et al. reported the human hatched embryo developed slowly and steadily without the collapse of TE until hatching was complete. Contrarily, the unhatched human embryo developed quickly, showed a number of blastocoel collapses, and finally degenerated. The number of collapses is significantly higher in unhatched human blastocysts [14]. Niimura et al. reported that strong collapse has the effect of inhibiting hatching in mouse embryos [23].

In our observation, mouse embryos cultured with GJis presented significant frequent collapses and devel opmental delay compared with controls (Table. 1). It is suggested that there is a relation between such embryonic morphological events and GJIC. GJIC dysfunction might induce embryonic collapses and might delay embryonic development, though many questions remain regarding the mechanism of collapse and hatching.

In conclusion, GJIC dysfunction leads to aberrant ICM division, frequent collapses, and developmental delay in mice. We were able to cause the aberrant behavior of mouse ICM, which has not been reported in mouse fresh embryos to date. This TLM observation shows that oleamide and heptanol are useful reagents for investigating the function of GJIC during ICM division without disturbing blastocyst formation.

References

1. Shirayoshi Y, Okada TS, Takeichi M. The calcium-dependent cell-cell adhesion system regulates inner cell mass formation and cell surface polarization in early mouse development. Cell. 1983;35:631–8.
2. Nishioka N, Inoue K, Adachi K, Kiyonari H, Ota M, Ralston A, et al. The Hippo signaling pathway components Lats and Yap pattern Tead4 activity to distinguish mouse trophectoderm from inner cell mass. Dev Cell. 2009;16:398–410.
3. Zhou JZ, Jiang JX. Gap junction and hemichannel-independent actions of connexins on cell and tissue functions – An update. FEBS Lett. 2014;588:1186–92.
4. Houghton FD. Role of gap junctions during early embryo development. Reproduction. 2005;129:129–35.
5. Houghton FD, Barr KJ, Walter G, Gabriel HD, Grümmer R, Traub O, et al. Functional significance of Gap junctional coupling in pre-implantation development. Biol Reprod. 2002;66:1403–12.
6. Bloor DJ, Wilson Y, Kibschull M, Traub O, Leese HJ, Winterhager E, et al. Expression of connexins in human preimplantation embryos in vitro. Reprod Biol Endocrinol. 2004;2:25.
7. Harris A., Locke D. Connexins: A Guide. Humana Press, a part of Springer Science, New York, USA; 2009. pp 207–219, 270–271, 287–301.
8. Oyamada M, Takebe K, Endo A, Hara S, Oyamada Y. Connexin expression and gap-junctional intercellular communication in ES cells and iPS cells. Front Pharmacol. 2013. doi:10.3389/fphar.2013.00085.
9. Lo CW, Gilula NB. Gap junctional communication in the preimplantation mouse embryo. Cell. 1979;18:399–409.
10. Becker DL, Leclerc-David C, Warner A. The relationship of gap junctions and compaction in the preimplantation mouse embryo. Dev Suppl.1992:113–118.
11. Becker DL, Davies CS. Role of gap junctions in the development of the preimplantation mouse embryo. Microsc Res Tech. 1995;31:364–74.
12. Vance MM, Wiley LM. Gap junction intercellular communication mediates the competitive cell proliferation disadvantage of irradiated mouse preimplantation embryos in aggregation chimeras. Radiat Res. 1999;152:544–51.
13. Mio Y, Maeda K. Time-lapse cinematography of dynamic changes occurring during in vitro development of human embryos. Am J Obstet Gynecol. 2008;199:660.e1–5. doi:10.1016/j.ajog.2008.07.023.
14. Mio Y, Iwata K, Yumoto K, Maeda K. Human embryonic behavior observed with time-lapse cinematography. J Health Med Info. 2014;5:143. doi:10.4172/2157-7420.1000143.
15. Evans WH, Boitano S. Connexin mimetic peptides: specific inhibitors of gap-junctional intercellular communication. Biochem Soc Trans. 2001;29:606–12.
16. Cotrina ML, Lin JH, Alves-Rodrigues A, Liu S, Li J, Azmi-Ghadimi H, et al. Connexins regulate calcium signaling by controlling ATP release. Proc Natl Acad Sci U S A. 1998;95:15735–40.
17. Guan X, Cravatt BF, Ehring GR, Hall JE, Boger DL, Lerner RA, et al. The sleep-inducing lipid oleamide deconvolutes gap junction communication and calcium wave transmission in glial cells. J Cell Biol. 1997;139:1785–92.
18. Nelson WL, Makielski JC. Block of sodium current by heptanol in voltage-clamped canine cardiac Purkinje cells. Circ Res. 1991;68:977–83.
19. Mori T, Amano T, Shimizu H. Roles of gap junctional communication of cumulus cells in cytoplasmic maturation of porcine oocytes cultured in vitro. Biol Reprod. 2000;62:913–9.
20. Pan G, Thomson JA. Nanog works together with other key pluripotent factors such as Oct4 and Sox2 to control a set of target genes that have important functions in ES cell pluripotency. Cell Res. 2007;17:42–9.
21. Ke Q, Li L, Cai B, Liu C, Yang Y, Gao Y, et al. Connexin 43 is involved in the generation of human-induced pluripotent stem cells. Hum Mol Genet. 2013;22:2221–33.
22. Chen AA, Tan L, Suraj V, Reijo Pera R, Shen S. Biomarkers identified with time-lapse imaging discovery, validation, and practical application. Fertil Steril. 2013;99:1035–43.
23. Niimura S. Time-lapse videomicrographic analyses of contractions in mouse blastocysts. J Reprod Dev. 2003;49:413–23.